interval at Meishan occurs during the transition from the latest Permian Changhsing Formation to the Earliest Triassic Yinkeng Formation. The Changhsing Formation is composed of graded beds of organic-rich calcarenite, marly micrite, and radiolarian chert, representing slope-to-basinal facies (*13*). A third-order sequence boundary surface occurs 20 cm below the top of the Changhsing Formation, with the topmost 20 cm of lime mudstone (bed 24e) representing a shelf margin system tract. Bed 24e is overlain by a transitional sequence of about 28 cm with a sharp contact. It consists of a pale-colored, alternated ash clay bed (bed 25) below, a laminated organic-rich calcareous claystone (bed 26) in the middle, and a 16-cm lime mud bed above (bed 27). Bed 26 contains rare but highly diverse skeletal fossils, including the earliest Triassic ammonoid *Otoceras*. Bed 27 includes an extensively burrowed hardground 5 cm above its base and discontinuous hardgrounds in its upper part (*16*). The first occurrence of the conodont *Hindeodus parvus* between bed 27c and bed 27b at section D of Meishan has been proposed as the biostratigraphic P-T boundary. Overlying the transitional sequence are graded beds ranging from gray organic-rich shale to pale marls or muddy limestone. The earliest postulated extinction event (*7, 8*) is referred the elimination of latest Permian reefs in South China, which corresponds to the base of bed24e at Meishan. The second event is the disappearance of most benthos at beds 25 and 26, and the final event is the disappearance of the final few Permian brachiopods at bed 28.

13. P. B. Wignall and A. Hallam, *Palaeogeogr. Palaeoclimatol. Palaeoecol.* **102**, 215 (1993).
14. M. S. Springer, *Paleobiology* **16**, 512 (1990). Confidence intervals on the apparent stratigraphic range of selected taxa were calculated from $C_1 = 1 - (1 + r/R)^{-(H-1)}$, where C_1 is the confidence level, r is the size of the confidence interval, R is the observed stratigraphic range, and H is the number of known fossil horizons (*12*). Because confidence intervals with $H < 2$ would be of little value, 59 genera with single occurrences were excluded, as were four foraminiferal and six conodont genera ranging throughout the section. The predicted positions of the true extinction horizons for 93 genera and for foraminifer, ostracod, and brachiopod genera, assuming there is one for each case, were computed separately. All genera with confidence values higher than 95% for disappearance well below the bottom of bed 24 (the boundary level) were eliminated. Using the binomial distribution, we calculated the 99% confidence envelope and eliminated genera with confidence intervals beyond the envelope. This process was repeated for the remaining genera, with the predicted true extinction horizon lying between the intervals.
15. K. H. Meldahl, *Geology* **18**, 890 (1990).
16. C. Q. Cao and Q. H. Shang, *Palaeoworld* **9**, 147 (1998).
17. The predicted true extinction level before 251.4 Ma is at 252.6 Ma with 96% confidence for a 0.6-My spacing but only 46.8% for a 0.1-My spacing.
18. W. C. Hao, *J. Geosci. Osaka City Univ.* **39**, 19 (1994).
19. S. Ouyang and J. Utting, *Rev. Palaeobot. Palynol.* **66**, 65 (1990).
20. Z. Yan, D. Xu, L. F. Ye, R. M. Lu, *Palaeoworld* **1**, 113 (1989).
21. Twenty-milligram samples were recovered with a microdriller for each point and were reacted with 100% H_3PO_4 at 25°C for 8 hours. Samples were analyzed in a Finnegan MAT 251 mass spectrometer for $\delta^{13}C$ and $\delta^{18}O$, using the Chinese national standard, an Ordovician carbonate from a site near Beijing [reference number GBW 04405: $\delta^{13}C = 0.57 \pm 0.03$ Pee Dee belemnite (PDB); $\delta^{18}O = -8.49 \pm 0.13$ PDB]. Analysis of a weathered specimen from bed 27 produced $\delta^{13}C$ values ranging from −3.6 to −4.2‰ and $\delta^{18}O$ values ranging from −8.2 to 12.6‰.
22. F. Asaro, L. W. Alvarez, W. Alvarez, H. V. Michel, *Geol. Soc. Am. Spec. Pap.* **190**, 517 (1982).
23. Z. G. Gao, D. Y. Xu, Q. W. Zhang, Y. Y. Sun, *Geol. Rev.* **33**, 203 (1987). Microspherules from boundary clay beds range from 50 to 300 μm, and most average 100 μm in diameter. Ninety-five percent are spherical; a few are oval, teardrop-shaped, or consist of two fused spheres. Ninety percent are ferruginous, black, metallic, and strongly magnetic, with delicate surface projections. X-ray analysis suggests that they are possibly composed of magnesioferrite and hematite, but one spherule is chromespinel (*7*). Ten percent are glassy and range from colorless to yellowish, brownish, or semitransparent. These sperules are isotropic in polarized light, with smooth, individually reticulate, or pitted surfaces. No phenocrysts or microliths of high-temperature minerals have been found in the glassy spherules. Both kinds of spherules may bear vesicles. Microprobe analysis indicates less than 0.1% Cr_2O_3, SO_3, and NiO in both kinds of spherules. Glassy spherules contain SiO_2, 34.6 to 54.9%; Al_2O_3, 4.9 to 17.8%; FeO, 4.8 to 11.0%; CaO, 11.5 to 36.1%; and MgO, 0.5 to 3.0%. Ferruginous spherules contain SiO_2, 48.0 to 29.5%; Al_2O_3, 15.8 to 22.7%; FeO, 40.9 to 80.3%; CaO, 0.7 to 2.7%; and MgO, 1.2 to 3.1%. In ferruginous spherules, amounts of SiO_2 and CaO are lower than in glassy spherules, and K_2O is entirely absent.
24. K. X. Zhang *et al.*, in *The Palaeozoic-Mesozoic Boundary*, H. F. Yin, Ed. (China Univ. of Geology Press, Wuhan, 1996).
25. C. Q. Cao, thesis, Nanjing Institute of Geology and Palaeontology, Nanjing, China (1999).
26. J. W. He, L. Rui, C. F. Chai, S. L. Ma, *J. Stratigr.* **11**, 194 (1987).
27. H. Visscher *et al.*, *Proc. Natl. Acad. Sci. U.S.A.* **93**, 2155 (1996).
28. S. D'Hondt, personal communication.
29. We appreciate discussions and comments from S. D'Hondt and C. Marshall and comparative $\delta^{13}C$ data from S. D'Hondt. Supported by the NSF China Grant 49672092, the Ministry of Science and Technology China Basic Research Projects G99-A-05b and G2000077705, Academia Sinica grant K2951-B1-409, and the NASA Exobiology Program and National Astrobiology Institute (to D.H.E.).

21 March 2000; accepted 30 May 2000

Negative Regulation of the *SHATTERPROOF* Genes by FRUITFULL During *Arabidopsis* Fruit Development

Cristina Ferrándiz,* Sarah J. Liljegren,* Martin F. Yanofsky†

The terminal step of fruit development in *Arabidopsis* involves valve separation from the replum allowing seed dispersal. This process requires the activities of the *SHATTERPROOF* MADS-box genes, which promote dehiscence zone differentiation at the valve/replum boundary. Here we show that the *FRUITFULL* MADS-box gene, which is necessary for fruit valve differentiation, is a negative regulator of *SHATTERPROOF* expression and that constitutive expression of *FRUITFULL* is sufficient to prevent formation of the dehiscence zone. Our studies suggest that ectopic expression of *FRUITFULL* may directly allow the control of pod shatter in oilseed crops such as canola.

The fruit mediates the maturation and dispersal of seeds and is derived from the female reproductive structure, the gynoecium. The *Arabidopsis* fruit, which is typical of more than 3000 species of *Brassicaceae*, consists of an apical stigma, a short style, and a basal ovary that contains the developing seeds (Fig. 1A). The peripheral walls of the fruit are referred to as valves and are connected on both sides by a thin structure known as the replum. At the valve/replum boundary, a narrow band of cells differentiates into the dehiscence zone (*1*), where the separation of cells late in fruit development allows valve detachment from the replum and seed dispersal.

Because *FRUITFULL* (*FUL*) is required for the expansion and differentiation of fruit valves after fertilization (*2*), we generated transgenic plants in which *FUL* is constitutively expressed from the cauliflower mosaic virus 35*S* promoter (*3–5*) to determine if *FUL* is sufficient to specify valve cell fate in ectopic positions. The most striking phenotype caused by the 35S::FUL transgene is the conversion of cells within the valve margin and outer replum to valve cells (Fig. 1). Consequently, the dehiscence zone, which normally forms at the valve margin (Fig. 1, A and C), fails to differentiate in 35S::FUL fruit (Fig. 1, B and D). Thus, like *shatterproof* (*shp1 shp2*) loss-of-function mutants (*6*), 35S::FUL gain-of-function plants produce indehiscent fruit and fail to disperse their seeds normally.

Because lignification is thought to play an important role in the dehiscence process (*1*), and because the *SHP* genes promote lignification of cells adjacent to the dehiscence zone (*6*), we examined the lignification patterns of 35S::FUL and *ful* fruit compared with that seen in the wild type (*7*). Whereas only a single valve cell layer is lignified in wild-type fruit (Fig. 1E), all of the internal valve mesophyll layers also become lignified in *ful* fruit (Fig. 1G). Correspondingly, in 35S::FUL fruit (Fig. 1F), we found a consis-

Section of Cell and Developmental Biology, University of California at San Diego, La Jolla, CA 92093–0116, USA.

*These authors contributed equally to this work.
†To whom correspondence should be addressed. E-mail: marty@ucsd.edu

tent loss of lignified cells adjacent to where the dehiscence zone normally forms. Therefore, *FUL* is necessary to prevent ectopic lignification of certain valve cells, and constitutive expression of *FUL* is sufficient to prevent valve margin lignification.

The similarities between the indehiscent phenotypes of 35S::FUL and *shp1 shp2* fruit, together with the complementary expression patterns of *FUL* and *SHP* (*3*, *8*, *9*), suggest either that *FUL* negatively regulates *SHP1/2*, that *SHP1/2* negatively regulate *FUL*, or that *FUL* and *SHP1/2* repress each other. To determine if *FUL* is a negative regulator of the *SHP* genes, we compared the accumulation of *SHP* RNAs in wild-type, *ful*, and 35S::FUL fruit (*10*). We observed that the domains of *SHP1* (Fig. 2, A and B) and *SHP2* (*11*) expression expanded throughout the valves of *ful* fruit, and conversely, that *SHP* expression was down-regulated in 35S::FUL fruit (Fig. 2, C and D). Thus, FUL is a negative spatial regulator of *SHP* RNA accumulation. To determine if the *SHP* gene products negatively regulate *FUL*, we analyzed the expression pattern of *FUL* in wild-type, *shp1 shp2*, and 35S::SHP1/2 fruit (*10*). We found that the domain of *FUL* expression did not expand to include the valve margin regions of *shp1 shp2* fruit (Fig. 2, E and F), and that expression of the FUL::GUS marker was not down-regulated in 35S::SHP1/2 fruit (Fig. 2, G and H). Therefore, SHP1/2 do not negatively regulate *FUL* RNA accumulation.

The observation that *SHP1/2* are ectopically expressed throughout the valves of *ful* mutants suggested that some of the *ful* mutant phenotypes could be due to ectopic *SHP* activity. To investigate this possibility, we compared *shp1 shp2 ful* fruit (*12*) to *ful* fruit (Fig. 3). While they appeared very similar (Fig. 3A), *shp1 shp2 ful* fruit exhibited tears in the valves due to seed crowding (Fig. 3, B and C) less frequently, had guard cells in the valve outer epidermis (Fig. 3, D to F), and were indehiscent. Although *SHP* activity promotes valve margin lignification (*6*), the valves of *shp1 shp2 ful* fruit are still ectopically lignified (*11*), indicating that ectopic *SHP* activity is not primarily responsible for this and other *ful* mutant phenotypes.

To identify additional genes regulated by *FUL* that may contribute to *ful* phenotypes, we analyzed expression of the valve margin marker GT140 (*13*, *14*) in *ful* and 35S::FUL fruit compared with expression in the wild type. Whereas GT140 is normally expressed in narrow stripes at the valve margin (Fig. 2I), this marker was ectopically expressed throughout *ful* mutant valves (Fig. 2J) and was largely absent in 35S::FUL fruit (Fig. 2K). Because *SHP* activity is required for GT140 valve margin expression (*6*), and *SHP* expression also expands throughout *ful* valves and is down-regulated in 35S::FUL fruit, ectopic GT140 expression in *ful* fruit could be entirely due to ectopic *SHP* activity. To investigate this possibility, we also analyzed expression of the GT140 marker in *shp1 shp2 ful* fruit. GT140 was still expressed throughout the triple-mutant valves (Fig. 2L), although at a reduced level relative to that seen in *ful* valves (Fig. 2J). These data suggest that FUL negatively regulates GT140 expression and demonstrate that *SHP* activity is not abso-

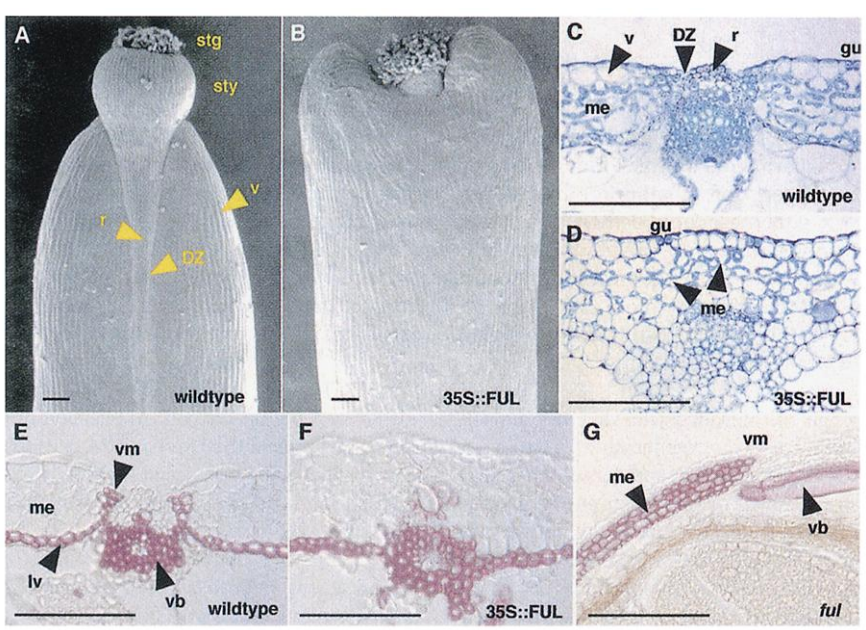

Fig. 1. Constitutive expression of *FUL* converts cells of the valve margin and outer replum into valve cells. Scanning electron micrographs (**A** and **B**) and transverse sections of fruit stained with toluidine blue (**C** and **D**) or phloroglucinol (**E** to **G**) at stage 17 (A to F) or stage 18 (G). In wild-type fruit (A, C, and E), cells at the valve margin differentiate into the dehiscence zone (DZ), and lignification of the valve inner subepidermal layer (lv) and small patches of valve margin cells (vm) adjacent to the dehiscence zone occurs. 35S::FUL fruit (B and D) have reduced styles (sty) and appear radially uniform, as cells within the valve margin and outer replum (r) regions closely resemble wild-type valve (v) cells. Because of these cell fate conversions, dehiscence zone differentiation and valve margin lignification do not occur in 35S::FUL fruit (D and F). In contrast, *ful* fruit (G) show ectopic lignification of the valve mesophyll (me) layers; stg, stigma; gu, guard cells; vb, vascular bundle. Bars, 100 μm.

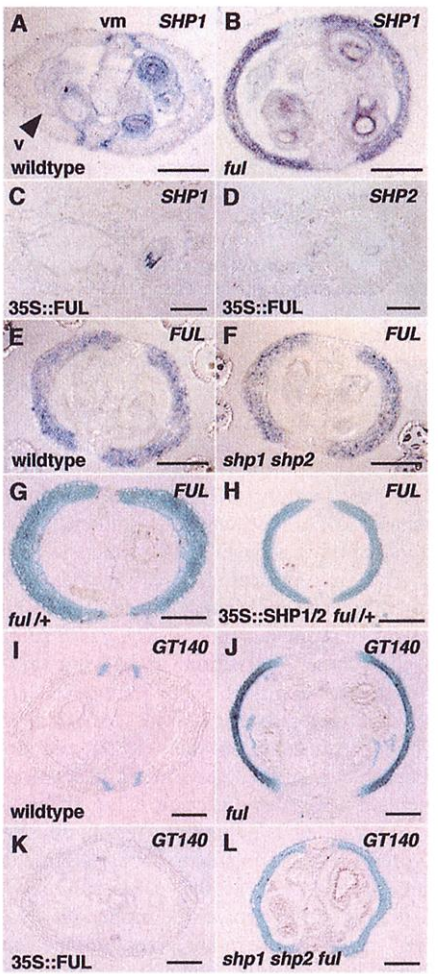

Fig. 2. FUL negatively regulates *SHP* and GT140 expression. Expression of *SHP1* (**A** to **C**), *SHP2* (**D**), *FUL* (**E** to **H**), and the GT140 valve margin marker (**I** to **L**) was analyzed by in situ hybridization (A to F) or by GUS reporter detection (G to L) in transverse sections of developing fruit at stage 13 (E and F), stage 15 (A to D), stage 16 (G to I and K), and stage 17 (J and L). In wild-type fruit, *SHP1* (A), *SHP2* (*11*), and GT140 (I) are expressed in stripes at the valve margin (vm) where the dehiscence zone will form. Expression of *SHP1*, *SHP2*, and GT140 expands throughout the valves (v) of *ful-2* fruit [B, J, and (*11*)] and is not detected in 35S::FUL fruit (C, D, and K). In *shp1 shp2 ful-2* fruit (L), expression of GT140 is detected throughout the valves at reduced levels. *FUL* is expressed in wild-type fruit valves (E) and does not expand beyond the valves of *shp1 shp2* fruit (F). In 35S::SHP1 35S::SHP2 *ful-1*/+ fruit (H), FUL::GUS expression does not appear reduced as compared with that seen in *ful-1*/+ fruit valves (G). Bars, 100 μm.

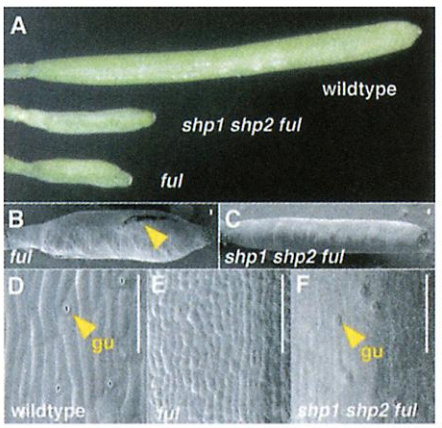

Fig. 3. Mutations in *SHP1* and *SHP2* partially suppress the valve differentiation defects of *ful* fruit and largely eliminate valve tearing. (**A**) Like *ful-1* fruit, *shp1 shp2 ful-1* fruit (stage 17) are much shorter than the wild type, due to the lack of valve expansion after fertilization. Valve tears (arrowhead) are present in nearly all *ful-1* fruit (**B**) and are rarely seen in *shp1 shp2 ful-1* fruit (**C**). Guard cells (gu) are present in wild-type and *shp1 shp2 ful-1* fruit valves (**D** and **F**) and are not found in *ful-1* fruit valves (**E**). Bars, 100 μm.

lutely required for GT140 expression in *ful* mutant valves, indicating that additional genes are involved in activating this marker.

The data presented here, together with other recently published observations, allow us to propose a model (Fig. 4) for some of the genetic interactions underlying valve margin development. The *SHP* genes are positively regulated by the *AGAMOUS* MADS-box gene product (*8*, *9*) and are required for proper valve margin development (*6*). Besides directing valve differentiation (*2*), FUL negatively regulates *SHP* expression, ensuring that valve margin cell fate occurs only at the valve boundary. Although not shown in the model, SHP1/2 may negatively regulate a replum-specific factor; expansion of such a factor's activity in *shp1 shp2* fruit could account for the observed slight restriction of *FUL* valve expression (Fig. 2, E and F). Expression of the GT140 valve margin marker is positively regulated by SHP1/2 (*6*) and negatively regulated by FUL, which may occur by way of an additional factor (factor X) involved in GT140 activation.

Fig. 4. Genetic interactions involved in valve margin development.

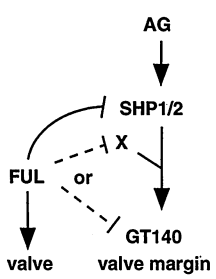

References and Notes

1. J. Spence, Y. Vercher, P. Gates, N. Harris, *J. Microsc.* **181**, 195 (1996).
2. Q. Gu, C. Ferrándiz, M. Yanofsky, R. Martienssen, *Development* **125**, 1509 (1998).
3. A. M. Mandel and M. F. Yanofsky, *Plant Cell* **7**, 1763 (1995).
4. P. N. Benfey and N. -H. Chua, *Science* **250**, 959 (1990).
5. The *FUL* cDNA was cloned into the pBIN-JIT vector, a pBIN19 (Clontech) derivative, which placed *FUL* transcription under the control of a tandem repeat of the 35S promoter. Eighteen of 28 independent transformants in the Columbia (Col) ecotype had similar phenotypes, and two lines (CFM5088 and CFM5092) were selected for further study. In addition to the phenotypes described, 35S::FUL plants flowered early, produced terminal flowers, and showed a threefold increase in seed weight.
6. S. J. Liljegren *et al.*, *Nature* **404**, 766 (2000).
7. Microscopy, tissue fixation, and histology were as described (*2*, *6*). Plastic sections (1 μm) are shown in Fig. 1, C and D, and paraplast sections (8 or 10 μm) are shown elsewhere.
8. B. Savidge, S. D. Rounsley, M. F. Yanofsky, *Plant Cell* **7**, 721 (1995).
9. C. A. Flanagan, Y. Hu, H. Ma, *Plant J.* **10**, 343 (1996).
10. RNA in situ hybridizations of wild-type (Col), *ful-2* (*15*), 35S::FUL, and *shp1-1 shp2-1* sections were done as described (*15*) with the *SHP1* (*9*), *SHP2* (*8*), and *FUL* (*3*) probes. 35S::SHP1/2 plants (*6*) were crossed to *ful-1* mutants (*2*), because a β-glucuronidase (GUS)–containing enhancer trap element inserted in the 5′-untranslated region behaves as an accurate reporter of *FUL* expression in *ful-1*/+ plants. GUS assays of 35S::SHP1/2 *ful-1*/+ fruit were as described (*6*).
11. C. Ferrándiz, S. Liljegren, M. Yanofsky, data not shown.
12. *shp1 shp2 ful-1* and *shp1 shp2 ful-2* fruit were compared with *ful-1* and *ful-2* fruit, respectively. Fruit lengths (in millimeters; $n = 30$) at stage 18 were as follows: wild type (Landsberg *erecta*), 14.2 ± 0.4; *ful-1*, 3.9 ± 0.1; *shp1 shp2 ful-1*, 4.1 ± 0.2; wild type (Col), 16.5 ± 0.5; *ful-2*, 5.6 ± 0.5; *shp1 shp2 ful-2*, 7.2 ± 0.5. Valve tears were present in 91.0% of *ful-1*, 2.5% of *shp1 shp2 ful-1*, and 0% of wild-type fruit ($n \geq 79$, stages 17 to 19). Stomata were also observed in *shp1 shp2 ful-2* fruit valves.
13. V. Sundaresan *et al.*, *Genes Dev.* **9**, 1797 (1995).
14. Plants carrying the GT140 marker were crossed to *ful-2*, *shp1 shp2 ful-2*, and 35S::FUL plants, and GUS assays were as described (*6*).
15. C. Ferrándiz, Q. Gu, R. Martienssen, M. F. Yanofsky, *Development* **127**, 725 (2000).

16. We thank A. Chen, S. Guimil, T. Kawashiwa, T. Khammungkhune, T. Kuhlmann, and C. Wiley for technical assistance. Supported by grants from the National Science Foundation.

11 April 2000; accepted 26 May 2000

Interdigital Regulation of Digit Identity and Homeotic Transformation by Modulated BMP Signaling

Randall D. Dahn and John F. Fallon*

The developmental mechanisms specifying digital identity have attracted 30 years of intense interest, but still remain poorly understood. Here, through experiments on chick foot development, we show digital identity is not a fixed property of digital primordia. Rather, digital identity is specified by the interdigital mesoderm, demonstrating a patterning function for this tissue before its regression. More posterior interdigits specify more posterior digital identities, and each primordium will develop in accordance with the most posterior cues received. Furthermore, inhibition of interdigital bone morphogenetic protein (BMP) signaling can transform digit identity, suggesting a role for BMPs in this process.

Although the signaling pathways that broadly establish polarity along the three axes of the developing limb bud are rapidly being elucidated (*1*), the downstream mechanisms that exquisitely pattern adult morphology are not well understood. For instance, in the developing chick limb bud the posterior mesodermal zone of polarizing activity (ZPA) controls anteroposterior (A/P) polarity through expression of the *Sonic hedgehog* (*Shh*) gene (*2*). However, the mechanisms by which early asymmetry is translated into the characteristic differences in phalangeal number and morphology that define digital identity are not understood. Application of ectopic SHH protein (SHH-N) or ZPA cells to the anterior border of early-stage limb buds elicits mirror-image patterns of digit duplication in a dose- and time-dependent manner (*2*, *3*). A recent report suggests that in the early limb bud, SHH acts long range to control digit number and short range to establish a BMP2 morphogen gradient that specifies digit identity in a dose-dependent fashion by progressively promoting anterior digital precursors to more posterior identities (*4*). This hypothesis implies that A/P positional value is specified during early limb bud stages under direct SHH influence and, by the time digital rays are forming, A/P positional value is a fixed property of digital primordia. Here, we employ both embryological and molecular methodologies to demonstrate that the

Department of Anatomy, University of Wisconsin, 1300 University Avenue, Madison, WI 53706, USA.

*To whom correspondence should be addressed. E-mail: jffallon@facstaff.wisc.edu